NUCL SCI TECH (2018) 29:27
https://doi.org/10.1007/s41365-018-0360-x

γ-Ray radiolysis of acetohydroxamic acid in HNO_3 and its radiolytic product

Jin-Hua Wang[1] · Chao Li[1] · Qian Li[1] · Ming-Hong Wu[1] · Wei-Fang Zheng[2] · Hui He[2]

Received: 18 January 2017 / Revised: 24 May 2017 / Accepted: 11 June 2017 / Published online: 6 February 2018

Abstract Acetohydroxamic acid (AHA) is a novel salt-free reagent used for the separation of Pu and Np from U in the advanced Purex process. This paper reports the γ-ray damage of AHA in HNO_3 and its radiolytic product. For 0.2 mol L^{-1} AHA in 0.2–2.0 mol L^{-1} HNO_3 irradiated at a dose of 5–25 kGy, the radiolytic rate of AHA is 6.63–77.5%, and it increases with the HNO_3 concentration and absorbed dose. The main radiolytic gases are N_2O and H_2, with volume fractions of $(0.500–16.2) \times 10^{-2}$ and $(1.30–11.8) \times 10^{-3}$, respectively, and they increase with the absorbed dose; the H_2 volume fraction decreases with increasing HNO_3 concentration. The main liquid radiolytic products are CH_3COOH and HNO_2, and their concentrations are $(3.40–19.7) \times 10^{-2}$ and $(0.200–4.80) \times 10^{-3}$ mol L^{-1}, respectively, which increase with the HNO_3 concentration. Since a significant concentration of HNO_2 is present in the irradiated AHA-HNO_3 solution, a holding reductant must be used to destroy HNO_2 and stabilize Pu(III) and Np(V) when AHA is applied for the separation of Pu and Np from U.

Keywords Acetohydroxamic acid · γ-Ray radiolysis · Radiolytic product · Complexant reductant · Purex process

✉ Jin-Hua Wang
jinhuawang@staff.shu.edu.cn

✉ Wei-Fang Zheng
wfazh@ciae.ac.cn

[1] School of Environmental and Chemical Engineering, Shanghai University, 99 Shangda Road, Shanghai 200444, China

[2] Radiochemistry Department, China Institute of Atomic Energy, Box 275, Beijing 102413, China

1 Introduction

In order to realize a closed nuclear fuel cycle, the spent fuel discharged from nuclear power reactors must be reprocessed for isolating and recycling the unburned U and Pu generated. In the partition cycle of the improved Purex process used for the reprocessing of spent fuel, both Pu and Np are expected to be separated from U. On the other hand, U purification also involves the removal of Pu and Np. Two methods have been proposed for the separation of Pu and Np from U: one is the reduction of Pu(IV) and Np(VI) to Pu(III) and Np(V), which are unextractable by tri-butyl-phosphate (TBP), the other is to complex Pu(IV) and Np(IV), while U(VI) is unaffected. In the partition cycle, the concentrations of Pu and Np are relative higher, and hence, an appropriate reductant or complexant can effectively separate these nuclides from U. In the U purification cycle, however, the Pu and Np contents are very low; thus, only a complexant would be effective for the decontamination of U from Pu and Np [1, 2]. A series of organic ligands, namely carboxymethylamine, formic acid, acetic acid, butyric acid, pyruvic acid, glycolic acid, formohydroxamic acid, acetohydroxamic acid (AHA), and *n*-propionyl-hydroxamic acid, were proposed and tested. The results showed that AHA is the best [2–6]. Many researchers studied the complexation of AHA with Pu(IV), Np(IV), and U(VI) [2–4, 7–11] and found that the stability constants for AHA-Pu(IV) and AHA-Np(IV) are much higher than that for AHA-U(VI). Therefore, AHA can preferentially strip Pu(IV) and Np(IV) from the TBP phase into the aqueous phase, while U(VI) is unaffected. In addition, AHA can rapidly reduce Np(VI) to Np(V); U(VI) is not reduced, but Pu(IV), after initial complex formation, is slowly reduced to Pu(III) [3, 12]. As AHA-Pu(IV),

AHA-Np(IV), Np(V), and Pu(III) are unextractable by TBP, Pu and Np can be well separated from U by AHA [5, 13–18]. AHA is composed of C, H, O, and N, and it can be completely incinerated to NO_2 and CO_2. Since no solid waste is generated by the addition of AHA [16], it is expected to be useful for the reprocessing of spent fuel. However, AHA might suffer from radiation damage during its use, which would affect its efficiency, and the resulting radiolytic products may hinder effective separation. Karraker [19] studied the radiolysis of AHA in HNO_3 at doses up to 11 kGy, which was estimated from the spent fuel to be reprocessed, and found that radiation decomposed a minor fraction of AHA compared to the loss by hydrolysis and that AHA radiolysis showed weak dependence on both the HNO_3 concentration and the absorbed dose. In his study, the residual AHA content was analyzed by the light absorption of an Fe(III)-AHA complex. However, he compared the effect of radiation damage on AHA based on the light absorption value of the diluted samples and not the residual concentration of AHA. As the irradiated samples were diluted 100–400 times, even a slight change in absorption may cause a significant difference in the AHA concentration, and the absorbance value obtained will not be representative of the AHA concentration; hence, these results are not reliable. In this study, the radiolysis of AHA is monitored based on the change in the AHA concentration, and the radiolytic product of AHA is also reported. These results are expected to serve as an important reference for the application of AHA in the reprocessing of spent fuel.

2 Experiment

2.1 Reagent

AHA was supplied by Aldrich Chemical Company, and its purity was 98%. Two kinds of standard gas mixtures were supplied by Shanghai Institute of Measurement and Testing Technology: one was composed of 2.50% hydrogen, 1.00% carbon monoxide, 1.00% carbon dioxide, 0.30% methane, 0.01% ethane, 0.01% ethene, and 95.18% nitrogen; the other contained 3.00% nitrous oxide and 97.00% nitrogen.

2.2 Main equipment and accessories

A 3.7×10^{15} Bq ^{60}Co-γ ray irradiator was supplied by Shanghai Institute of Applied Physics, Chinese Academy of Sciences. A T90 UV–VIS spectrophotometer was supplied by Beijing Purkinje General Instrument Co. Ltd. An ion chromatograph (research-style) was obtained from Switzerland Metrohm Co. Ltd. A GC900A gas chromatograph and a packed column with 5 Å molsieve (2 m × 3 mm) were supplied by Shanghai Ke Chuang Chromatograph Instruments Co. Ltd. A capillary column with aluminum oxide (50 m × 0.53 mm) was supplied by Lanzhou Institute of Chemistry and Physics, Chinese Academy of Sciences.

2.3 Sample preparation, irradiation, pretreatment, and analysis

0.2 mol L^{-1} AHA solutions containing different concentrations of HNO_3 were prepared as follows. A certain amount of AHA was put in a beaker, which was then placed in an ice-water bath. A certain amount of 0.5 mol L^{-1} HNO_3 was slowly dropped into the beaker with stirring, and then, a certain amount of slightly diluted HNO_3 was added. The solution was transferred to a 100-mL measuring flask to a constant volume. Thus, solutions in which the AHA concentration was 0.2 mol L^{-1} and the HNO_3 concentration was 0.2, 0.5, 1.0, and 2.0 mol L^{-1} were prepared. Four milliliters of each solution was placed in 7-mL glass vials, which were sealed with a sealing machine. The samples were irradiated by ^{60}Co γ-ray to 5, 10, 15, 20, and 25 kGy, and the absorbed doses were monitored by dichromate dosimeters. Control samples were used for comparison of the radiation effect on the loss of AHA by hydrolysis as well as on the amount of radiolytic product. The gases evolved from the irradiated AHA solutions were tested by gas chromatography for the analysis of H_2, N_2O, CH_4, and C_2H_6. The irradiated AHA solutions and control samples were neutralized by KOH solution and then diluted to the suitable concentrations. Finally, these pretreated samples were tested by ultraviolet–visible spectrophotometry and ion chromatography for the analysis of AHA, HCOOH, and HNO_2.

2.4 Analysis of AHA and its radiolytic products

Quantitative analysis of AHA was performed by ultraviolet–visible spectrophotometry. 2.7, 5.3, 8.0, and 10.7 m mol L^{-1} standard AHA solutions were prepared using high-purity water. 1.00 mL of each solution was placed in a 10-mL measuring flask, to which 3.00 mL $FeCl_3$ solution (10 wt%) and 4.00 mL CCl_3COOH solution (2.5 wt%) were separately added. Then, water was added to constant volume, and the solutions were shaken well. The reference solution was prepared in the same manner as the standard AHA solutions but without AHA. These standard AHA solutions were tested at 502 nm by using an ultraviolet–visible spectrophotometer. The response curve for AHA was obtained from the AHA concentrations and the corresponding absorbance. The irradiated AHA solutions and control samples were neutralized by KOH

solutions and diluted to suitable concentrations. These pretreated samples were tested by using the ultraviolet–visible spectrophotometer. From the response curve for AHA and the absorbance of the diluted samples, the residual AHA concentrations in the samples were calculated. H_2, N_2O, CH_4, and C_2H_6 were analyzed by gas chromatography. For H_2 analysis, a 5 Å molsieve packed column was used, and the column temperature was 80 °C; a thermal conductivity detector (TCD) was employed, and its temperature was 110 °C. The carrier gas was Ar, with a flow rate of 10 mL min^{-1}. N_2O analysis was conducted using a packed shincarbon T column and a TCD detector. H_2 was used as the carrier gas, and its flow rate was 25 mL min^{-1}. The column temperature was programmed as follows: initial temperature, 100 °C; initial isothermal period, 7 min; programmed heating rate, 35 °C min^{-1}; final temperature, 220 °C; and final isothermal period, 1 min. The TCD temperature was 120 °C. CH_4 and C_2H_6 were analyzed using a PLOT Al_2O_3 column and a flame ionization detector (FID). The carrier gas was N_2, and its flow rate was 19 mL min^{-1}. The column temperature was 40 °C, and the FID temperature was 110 °C. CH_3COOH and HNO_2 were analyzed by ion chromatography with an electric conductivity detector, using a METROSEP A SUPP 5–250 column. The eluent was a solution containing 3.2 mmol $L^{-1}Na_2CO_3$ and 1.0 mmol $L^{-1}NaHCO_3$, and its flow rate was 0.7 mL min^{-1}.

2.5 Formulae used in the paper

The hydrolysis rate of AHA is defined as follows: hydrolysis rate $= (C_0 - C_c)/C_0 \times 100\%$, where C_0 is the original AHA concentration and C_c is the AHA concentration in the control sample. The radiolysis rate of AHA is defined by the equation: radiolysis rate $= (C_c - C_i)/C_c \times 100\%$, where C_i is the AHA concentration in the irradiated sample. The volume fraction of the gas product is calculated as follows: if the response curve equation of a component is $y = ax + b$, the X axis is the injected volume of the standard gas mixture, and the Y axis is the corresponding peak area of the component. Then, the volume fraction of the component is calculated by the following formula: volume fraction $= (A - b)c/ae$, where A is the component peak area in the gas chromatogram of the gas sample, c is the volume fraction of the component in the standard gas mixture, and e is the injected volume of sample gas.

3 Results and discussion

3.1 Radiolysis of AHA in HNO_3 solution

As AHA can complex with Fe(III) in an acidic solution to yield a colored product, it can be analyzed by ultraviolet–visible spectrophotometry [15]. The response curve for AHA is $y = 114.38x + 0.0142$ (concentration range 2.70–10.7 m mol L^{-1}), and the correlation coefficient (R^2) is 0.9994. The AHA concentration in control samples decreases drastically with increasing HNO_3 concentration. When the HNO_3 concentration is 0, 0.2, 0.5, 1.0, and 2.0 mol L^{-1}, the hydrolysis rate of AHA is 8.20, 23.1, 41.2, 66.2, and 85.9%, respectively, indicating that the rate increases with the HNO_3 concentration. This result is consistent with that reported by Taylor [20] and Tkac [10]. In an acidic solution, AHA hydrolyzes to acetic acid and hydroxylamine:

$$CH_3CONHOH + H_2O + H^+ \rightarrow CH_3COOH + NH_3OH^+. \quad (1)$$

As the time lag among sample preparation, irradiation, and neutralization is very long (about 9 h), this observation cannot be used to elucidate the hydrolysis of AHA employed in the advanced Purex process. In the separation of Pu and Np from U by countercurrent liquid–liquid extraction, the residence time is about 30 min; if the separation occurs in the centrifugal contactor, the residence time is much shorter. We have studied the hydrolysis of AHA in HNO_3 at different times [21]. At 0.2 mol L^{-1} AHA, with 0.2, 0.5, 1.0, and 2.0 mol L^{-1} HNO_3, the hydrolysis rate of AHA at 0.5 h is 2.40, 5.30, 7.60, and 8.40, respectively; thus, the hydrolysis of AHA in 0.2–2.0 mol L^{-1} HNO_3 would not be drastic. In addition, fast complexation of AHA with a metal leads to slower hydrolysis and stabilization of AHA in solution [10], so the hydrolysis of AHA will not affect its application in the

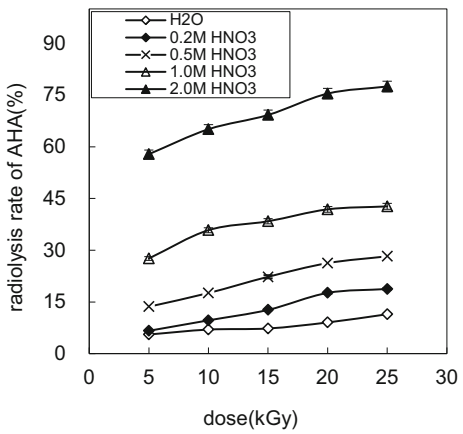

Fig. 1 Radiolysis rate of AHA as a function of dose

separation of Pu and Np from U. Figure 1 illustrates the radiolysis rate of AHA as a function of dose.

Figure 1 shows that the radiolysis rate of AHA is 6.63–77.5% in AHA solution irradiated to 5–25 kGy, and it increases with the dose and HNO_3 concentration. Karraker [19] reported that AHA radiolysis shows weak dependence on both HNO_3 concentration and absorbed dose, and this differs from our experimental results. When the dose is increased fivefold, from 5 to 25 kGy, the radiolysis rate increases 1.3–2.8 times. When the HNO_3 concentration is increased fivefold, from 0.2 to 1.0 mol L^{-1}, the radiolysis rates increases 2.3–4.2 times. Thus, the effect of HNO_3 concentration on the radiolysis of AHA is stronger than that of the dose. Water radiolyzes to produce ·OH, e_{aq}^{-1},·H, and so on:

$$H_2O \rightsquigarrow \bullet OH,\ e_{aq}^{-},\ \bullet H,\ H_2,\ H_2O_2,\ H_3O^{+}. \quad (2)$$

·OH may react with HNO_3 by H abstraction to form $\cdot NO_3$ [22]:

$$\cdot OH + HNO_3 \rightarrow \cdot NO_3 + H_2O. \quad (3)$$

When using 0.2–2.0 mol L^{-1} HNO_3, most of the acid dissociates to form NO_3^-. γ-Ray may react directly with HNO_3 and NO_3^- to produce $\cdot NO_3$ [23]:

$$NO_3^{-} \rightsquigarrow \bullet NO_3 + e^{-}, \quad (4)$$

$$HNO_3 \rightsquigarrow HNO_3^{+} + e^{-}, \quad (5)$$

$$HNO_3^{+} \rightarrow \cdot NO_3 + H^{+}, \quad (5^*)$$

·OH and $\cdot NO_3$ are oxidative radicals, and they may react with AHA as follows [24]:

$$\cdot OH + CH_3CONHOH \rightarrow CH_3CONHO\cdot + H_2O, \quad (6)$$

$$\cdot NO_3 + CH_3CONHOH \rightarrow CH_3CONHO\cdot + HNO_3. \quad (7)$$

Since the concentrations of ·OH and $\cdot NO_3$ increase with dose (Eqs. 2, 4–5*) and the $\cdot NO_3$ concentration increases with HNO_3 concentration (Eqs. 3–5*), the radiolysis rate increases with both dose and HNO_3 concentration.

3.2 Radiolytic product of AHA

HNO_3 ionizes to produce H^+, and e_{aq}^{-1} can react with H^+ to form H:

$$H^+ + e_{aq}^- \rightarrow \cdot H. \quad (8)$$

H· may react with AHA to form H_2:

$$\cdot H + CH_3CONHOH \rightarrow CH_3CONHO\cdot + H_2, \quad (9)$$

e_{aq}^- and ·H· may also react with NO_3^- generated from the ionization of HNO_3, as follows [22]:

$$\cdot H + NO_3^- \rightarrow HNO_3^- \rightarrow \cdot NO_2 + OH^-, \quad (10)$$

$$e_{aq}^- + NO_3^- \rightarrow NO_3^{2-}\ (+H_2O) \rightarrow \cdot NO_2 + 2OH^-. \quad (11)$$

Two $\cdot NO_2$ radicals may react with each other to form N_2O_4, which can react with water to produce HNO_2:

$$\cdot NO_2 + \cdot NO_2 \rightarrow N_2O_4\ (+H_2O) \rightarrow HNO_2 + HNO_3. \quad (12)$$

The C–C bond in the excited AHA molecule may be broken as follows [25]:

$$CH_3CONHOH \rightsquigarrow \bullet CH_3 + \bullet CONHOH. \quad (13)$$

$\cdot CH_3$ may react with AHA by H abstraction to form CH_4, or two $\cdot CH_3$ radicals may also react with each other to produce C_2H_6:

$$\cdot CH_3 + CH_3CONHOH \rightarrow CH_4 + CH_3CONHO, \quad (14)$$

$$\cdot CH_3 + \cdot CH_3 \rightarrow C_2H_6. \quad (15)$$

Two $CH_3CONHO\cdot$ radicals may react with each other to produce $CH_3CON{=}O$ [26]:

$$CH_3CONHO\cdot + CH_3CONHO\cdot \rightarrow CH_3CON{=}O + CH_3CONHOH\cdot \quad (16)$$

$CH_3CON{=}O$ may hydrolyze to form acetic acid and nitroxyl [27, 28]:

$$CH_3CON{=}O + H_2O \rightarrow CH_3COOH + HN{=}O. \quad (17)$$

Two nitroxyls can react with each other to generate N_2O:

$$HN{=}O + HN{=}O \rightarrow N_2O + H_2O. \quad (18)$$

Thus, the main radiolytic product of AHA in HNO_3 may be H_2, N_2O, CH_4, C_2H_6, CH_3COOH, and HNO_2.

3.2.1 H_2 generated by the radiolysis of AHA in HNO_3

H_2 was analyzed by gas chromatography using a packed 5 Å molsieve column and a TCD detector [29]. The response curve of H_2 is $y = 2297.8x + 48.87$ (volume range 0.100–1.20 mL), and R^2 is 1.000. The volume fraction of H_2 as a function of dose is shown in Fig. 2.

As shown in Fig. 2, the volume fraction of H_2 evolved from the AHA solutions irradiated with a dose of 5–25 kGy is (1.30–11.8) × 10^{-3}. The H_2 volume fraction increases with the dose but decreases with increased HNO_3 concentration. H_2 is produced by the reaction of H· and AHA (Eq. 9). H· is generated from the radiolysis of H_2O (Eq. 2), and it may also be produced by the reaction of H^+ and e_{aq}^- (Eq. 8). As the concentrations of H· and e_{aq}^- increase with

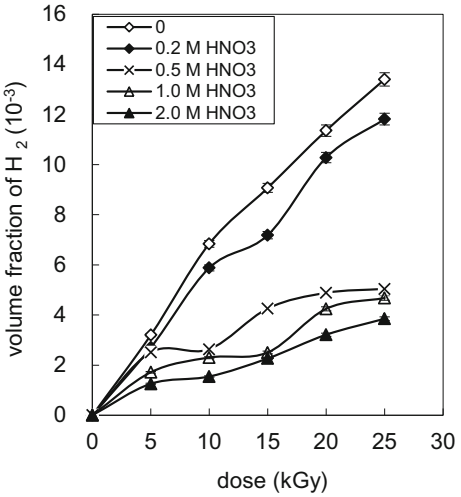

Fig. 2 Volume fraction of H_2 as a function of dose

the dose, the H_2 volume fraction also increases with increasing dose. Upon the addition of HNO_3, NO_3^- can react with ·H and e_{aq}^- (Eqs. 10–11), so that the ·H concentration is reduced; hence, the volume fraction of H_2 decreases with increased HNO_3 concentration.

3.2.2 N_2O generated from the radiolysis of AHA in HNO_3

We used gas chromatography with a packed shincarbon T column and a TCD detector to analyze N_2O. The response curve of N_2O is $y = 220.83x - 17.67$ (volume range 0.020–3.00 mL), and R^2 is 0.9933. The volume fraction of N_2O as a function of dose is shown in Fig. 3.

Figure 3 reveals that the volume fraction of N_2O produced from AHA solutions irradiated up to a dose of 5–25 kGy is (3.29 –16.2) × 10^{-2}. The N_2O volume fraction increases with the dose and with the HNO_3 concentration when the acid concentration is ≤ 0.5 mol L^{-1}. The dependence of the N_2O volume fraction on the HNO_3 concentration is not obvious when the acid concentration is higher than 0.5 mol L^{-1}. ·OH, $·NO_3$, ·H, and $·CH_3$ react with AHA to form $CH_3CONHO·$ (Eqs. 6–7, 9, 14), and two $CH_3CONHO·$ radicals react to produce $CH_3CON{=}O$ (Eq. 16). After hydrolysis, the HNO produced generates N_2O (Eqs. 17–18). Since the concentrations of ·OH, $·NO_3$, ·H, and $·CH_3$ increase with the dose (Eqs. 2–5, 13), the volume fraction of N_2O also increases with the dose. On the other hand, the higher the HNO_3 concentration, the higher is the concentration of $·NO_3$, $CH_3CONHO·$, $CH_3CON{=}O$, and HNO (Eqs. 3–5, 7, 16, 17). N_2O is produced by the reaction between two moieties of HNO (Eq. 18), and thus, the volume fraction of N_2O increases with HNO_3 concentration. However, as discussed above, the radiolysis rate of AHA increases with HNO_3 concentration, and the reduction of AHA concentration causes a decrease in the N_2O content (Eqs. 7, 16, 17). At higher HNO_3 concentration, The increase in N_2O content resulting from the increased HNO_3 concentration is balanced by the decrease in N_2O content due to the reduced AHA concentration; consequently, the volume fraction of N_2O changes very slightly at high HNO_3 concentrations.

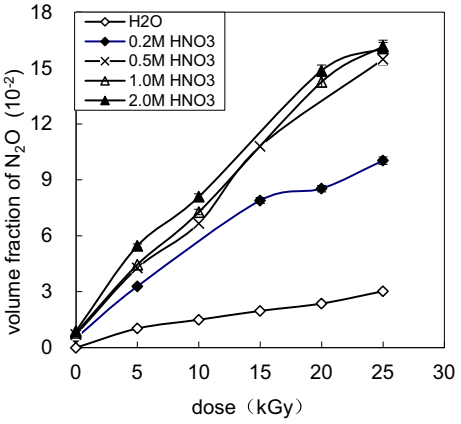

Fig. 3 Volume fraction of N_2O as a function of dose

3.2.3 CH_4 and C_2H_6 generated from radiolysis of AHA in HNO_3

CH_4 and C_2H_6 were analyzed by gas chromatography with a PLOT Al_2O_3 column and a FID detector [21]. The response curves of CH_4 and C_2H_6 are $y = 242.7x + 193.8$ and $y = 25.56x - 171.3$, respectively. The volume range is 2.0–200.0 μL, and the corresponding R^2 values are 0.9998 and 0.9956. The volume fractions of CH_4 and C_2H_6 evolved from AHA solutions irradiated up to 5–25 kGy are (1.90–47.4) × 10^{-5} and (0.200–1.00) × 10^{-5}, respectively; the volume fraction of CH_4 is much higher than that of C_2H_6. CH_4 is produced by the reaction of $·CH_3$ and AHA (Eq. 14), while C_2H_6 is generated by the reaction of two $·CH_3$ radicals (Eq. 15). As the concentration of AHA exceeds that of $·CH_3$, the volume fraction of CH_4 is much higher than that of C_2H_6.

Figure 4 shows that the volume fraction of CH_4 increases with the dose and with the HNO_3 concentration at HNO_3 ≤ 1.0 mol L^{-1}. When the HNO_3 concentration increases from 1.0 to 2.0 mol L^{-1}, there is no obvious change in the CH_4 volume fraction. CH_4 is generated by the reaction of $·CH_3$ and AHA (Eq. 14). The $·CH_3$ concentration increases with the dose, so the volume fraction of CH_4 also increases with the dose. $·CH_3$ may react with HNO_3 as below:

$$·CH_3 + HNO_3 \rightarrow CH_4 + NO_3· \quad (19)$$

Thus, the volume fraction of CH_4 increases with the HNO_3 concentration. However, the radiolysis rate of AHA

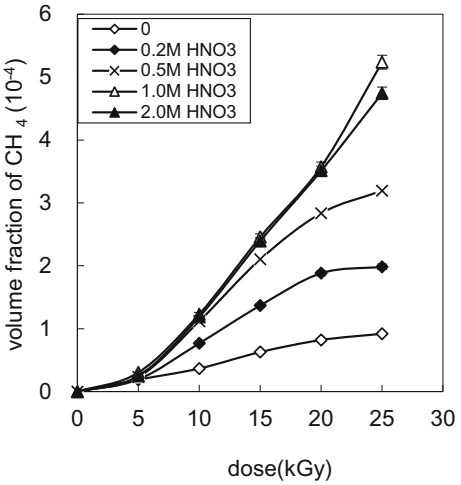

Fig. 4 Volume fraction of CH_4 as a function of dose

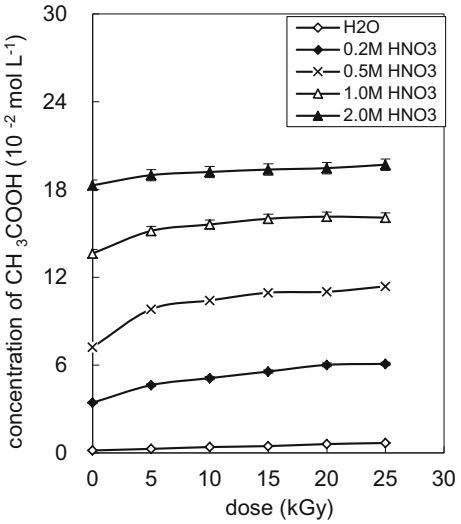

Fig. 5 CH_3COOH concentration as a function of dose

also increases with the HNO_3 concentration, as shown above, and the reduction of AHA concentration leads to a decrease in the CH_4 content (Eq. 14). At higher HNO_3 concentration, the reduction in CH_4 content caused by the decrease in AHA concentration is balanced by the increase in CH_4 content resulting from the increase in HNO_3 concentration; hence, the volume fraction of CH_4 changes slightly at high HNO_3 concentrations. The volume fractions of N_2O, H_2, CH_4, and C_2H_6 have the following relationship: $N_2O \approx 10\ H_2 \approx 150\ CH_4 \approx 7500\ C_2H_6$.

3.2.4 *CH_3COOH and HNO_2 generated by radiolysis of AHA in HNO_3*

Under alkaline conditions, CH_3COOH and HNO_2 can be converted into CH_3COO^- and NO_2^-, which can be analyzed by ion chromatography. The response curves of CH_3COOH and HNO_2 are $y = 872.97x$ and $y = 3766.1x$, respectively. The concentration range for CH_3COOH is 0.169–1.70 m mol L^{-1} and that for HNO_2 is 0.0217–0.435 m mol L^{-1}. The R^2 values for the response curves of CH_3COOH and HNO_2 are 0.9998 and 0.9984, respectively.

As shown in Fig. 5, the CH_3COOH concentration is $(4.64–19.7) \times 10^{-2}$ mol L^{-1} in AHA solutions irradiated up to 5–25 kGy. The CH_3COOH concentration increases markedly with HNO_3 concentration and slightly with the dose. ·OH, $\cdot NO_3$, ·H, and $\cdot CH_3$ react with AHA to form $CH_3CONHO\cdot$ (Eqs. 6–7, 9, 14); these radicals react with each other to produce $CH_3CON{=}O$ (Eq. 16), which in turn hydrolyzes to produce CH_3COOH (Eq. 17). Since the concentration of ·OH, $\cdot NO_3$, ·H, and $\cdot CH_3$ increases with the dose (Eqs. 2–5, 13), the CH_3COOH concentration also increases with the dose. When the HNO_3 concentration is high, the concentration of $\cdot NO_3$, $CH_3CONHO\cdot$, and $CH_3CON{=}O$ (Eqs. 3–5, 7, 16) also increases, as does the concentration of CH_3COOH (Eq. 17). For this reason, the CH_3COOH concentration increases with HNO_3 concentration.

Figure 6 reveals that the HNO_2 concentration is $(0.321–4.80) \times 10^{-3}$ mol L^{-1} in AHA solutions irradiated at a dose of 5–25 kGy; the concentration of HNO_2 increases with increasing concentration of HNO_3. When the HNO_3 concentration is ≤ 1.0 mol L^{-1}, the dependence of the HNO_2 concentration on the dose is not obvious. At a HNO_3 concentration of 2.0 mol L^{-1}, the HNO_2 concentration increases with the dose at lower dose levels, reaching the maximum value at 15 kGy, and then decreases with a further increase in the dose but changes only slightly beyond 20 kGy. Some papers [27, 29, 30] reported that AHA can react with HNO_2 and can scavenge HNO_2 and stabilize Pu(III) and Np(V); thus, an additional holding reductant is unnecessary [17]. The above-mentioned results

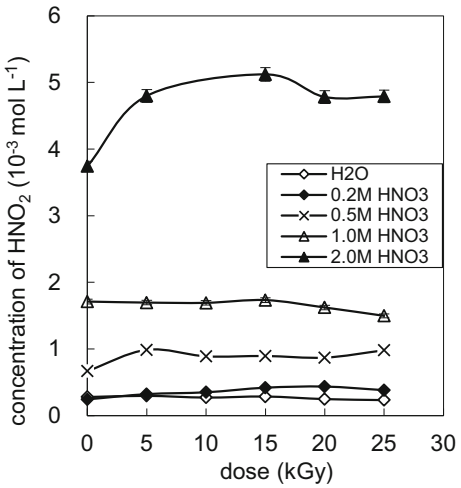

Fig. 6 HNO_2 concentration as a function of dose

show that a significant concentration of HNO_2 exists in the irradiated AHA-HNO_3 solution; this means that AHA cannot effectively destroy HNO_2, so a holding reductant should be used when AHA is applied for the separation of Pu and Np from U.

4 Conclusion

AHA is a potential complexant and reductant used in the separation of Pu and Np from U in the advanced Purex process for the reprocessing of spent fuel. The radiation stability of AHA in HNO_3 depends on the absorbed dose and HNO_3 concentration, but the effect of the latter is greater than that of the former. At a dose of 5–25 kGy, 0.2 mol L^{-1} AHA is recommended for use in HNO_3 with concentrations lower than 0.5 mol L^{-1}, where the radiolytic rate of AHA is lower than 29%. The use of AHA with 2.0 mol L^{-1} HNO_3 should be avoided, as the radiolytic rate of AHA is higher than 57%. The main gaseous products are N_2O and H_2, and the volume fraction of N_2O is higher than that of H_2. The main liquid products are CH_3COOH and HNO_2, and the concentration of the former is much higher than that of the latter. As HNO_2 will affect the stability of Pu(III) and Np(V), a holding reductant should be applied to scavenge HNO_2 when AHA is used for the separation Pu and Np from U. The effect of the holding reductant on the destruction of HNO_2, as well as on the stabilization of AHA and the radiolytic product of AHA in HNO_3, will be studied in the near future.

References

1. G.A. Ye, Review on the study and application of organic salt-free reagent in Purex process. At. Energy Sci. Technol. **38**, 152–158 (2004)
2. W.F. Zheng, L.M. Liu, Z. Chang, Improvement of separation of Pu from U of U-cycle in Purex process by acetohydroxamic acid. At. Energy Sci. Technol. **34**, 110–115 (2000)
3. R.J. Taylor, I. May, The reduction of actinide ions by hydroxamic acid. Czechoslovak J. Phys. **49**(Suppl. S1), 617–621 (1999). https://doi.org/10.1007/s10582-999-1041-0
4. I. May, R.J. Taylor, G. Brown, The formation of hydrophilic Np(IV) complexes and their potential application in nuclear fuel reprocessing. J. Alloys Compd. **271–273**, 650–653 (1998). https://doi.org/10.1016/S0925-8388(98)00179-0
5. H. Jiang, Z. Chang, Y.J. Pan et al., Effect of hydroxamic acid ligands on the extraction of plutonium by TBP. J. Nucl. Radiochem. **22**, 1–7 (2000)
6. W.F. Zheng, H. Jiang, J.M. Zhu et al., Complexation, reduction and stripping of Pu(IV) by simple hydroxamic acid. J. Nucl. Radiochem. **25**, 65–68 (2003)
7. M.J. Carrott, O.D. Fox, C.J. Maher et al., Solvent extraction behavior of plutonium(IV) ions in the presence of simple hydroxamic acids. Solvent Extr Ion Exch **25**, 723–745 (2007). https://doi.org/10.1080/07366290701634560
8. S. Sukumar, P.K. Sharma, P. Govindan et al., Purification of uranium product from plutonium contamination using acetohydroxamic acid based process. J. Radioanal. Nucl. Chem. **295**, 191–196 (2013). https://doi.org/10.1007/s10967-012-1855-2
9. R.J. Taylor, S.I. Sinkov, G.R. Choppin et al., Solvent extraction behavior of neptunium(IV) ions between nitric acid and diluted 30% tri-butyl phosphate in the presence of simple hydroxamic acids. Solvent Extr. Ion Exch. **26**, 41–61 (2008). https://doi.org/10.1080/07366290701784159
10. P. Tkac, B. Matteson, J. Bruso et al., Complexation of uranium(VI) with acetohydroxamic acid. J. Radioanal. Nucl. Chem. **277**, 31–36 (2008). https://doi.org/10.1007/s10967-008-0705-8
11. W.F. Zheng, Z. Chang, Synthesis of acetohydroxamic acid and determination of stability constants of its complexes with Pu(IV) and Np(IV). J. Nucl. Radiochem. **23**, 2–6 (2001)
12. C. Li, T.H. Yan, Ch. Zuo et al., Kinetics of reductive stripping of Np(VI) by acetohydroxamic acid from 30% TBP/kerosene to nitrate medium using a high-speed stirred cell. Radiochim. Acta **103**, 627–634 (2015). https://doi.org/10.1515/ract-2014-2375
13. P. Govindan, S. Sukumar, R.V.S. Rao, Partitioning of uranium and plutonium by acetohydroxamic acid. Desalination **232**, 166–171 (2008). https://doi.org/10.1016/j.desal.2007.12.014
14. P. Tkac, A. Paulenova, G.F. Vandegrift et al., Distribution and identification of Pu(IV) species in tri-*n*-butyl phosphate/HNO_3 extraction system containing acetohydroxamic acid. J. Radioanal. Nucl. Chem. **280**, 339–342 (2009). https://doi.org/10.1007/s10967-009-0524-6
15. W.F. Zheng, Z.P. Zhang, Z. Lin et al., Study on separation of Np from U by acetohydroxamic acid in Purex process. Nucl. Sci. Eng. **21**(4), 369–374 (2001)
16. YCh. Dong, H.L. Eil, The effect of acetohydroxamic acid on the distribution of Np(IV) and Np(VI) between 30% TBP and nitric acid. J. Alloys Compd. **451**, 440–442 (2008). https://doi.org/10.1016/j.jallcom.2007.04.238
17. R.J. Taylor, I. May, A.L. Wallwork et al., The applications of formo- and aceto-hydroxamic acids in nuclear fuel reprocessing. J. Alloys Compd. **271–273**, 534–537 (1998). https://doi.org/10.1016/S0925-8388(98)00146-7
18. G. Bernier, M. Miguirditchian, E. Ameil et al., Hot test in mixer settlers of alpha barrier with AHA in PUREX process. Procedia Chem. **7**, 160–165 (2012). https://doi.org/10.1016/j.proche.2012.10.027
19. D.G. Karraker, *Radiation Chemistry of Acetohydroxamic Acid in the Urex Process*, WSRC-TR-2002-00283 (2002), pp. 1–8
20. R.J. Taylor, I. May, The reduction of actinide ions by hydroxamic acids. Czech J. Phys. **49**, 617–621 (1999). https://doi.org/10.1007/s10582-999-1041-0
21. X.J. Cao, J.H. Wang, Q. Li et al., Stability of acetohydroxamic acid in nitric acid. At. Energy Sci. Technol. **48**, 1933–1937 (2014). https://doi.org/10.7538/yzk.2014.48.11.1933
22. Y. Katsumura, P.Y. Jiang, R. Nagaishi, Pulse radiolysis study of aqueous nitric acid solutions. formation mechanism, yield and reactivity of NO_3 radical. J. Phys. Chem. **93**, 4435–4439 (1991). https://doi.org/10.1021/j100164a050
23. Y. Katsumura, *N-centered Radicals* (Wiley, New York, 1998), pp. 393–412
24. Y. Samuni, U. Samuni, S. Goldstein, The mechanism underlying nitroxyl and nitric oxide formation from hydroxamic acids. Biochim. Biophys. Acta **1820**, 1560–1566 (2012). https://doi.org/10.1016/j.bbagen.2012.05.006
25. H.Y. Cheng, C.L. Xiang, Y.H. Chen, Radiation stability of extractant (I)—comparison of isomer radiolytic product of tributylphosphate. At. Energy Sci. Technol. **7**, 767–773 (1964)

26. A. Samuni, S.J. Goldstein, One-electron oxidation of acetohydroxamic acid: the intermediacy of nitroxyl and peroxynitrite. Phys. Chem. A **115**(14), 3022–3028 (2011). https://doi.org/10.1021/jp201796q
27. F.N. Shirota, E.G. DeMaster, M.C. Lee et al., Generation of nitric oxide and possibly nitroxylby nitrosation of sulfohydroxamic acids and hydroxamic acids. Biol. Chem. **3**, 445–453 (1999). https://doi.org/10.1006/niox.1999.0257
28. M.M. Gutierrez, A.E. Almaraz, E. Bari et al., The HNO donor ability of hydroxamic acids upon oxidation with cyanoferrates(III). J. Coord. Chem. **68**, 3236–3246 (2015). https://doi.org/10.1080/00958972.2015.1068938
29. J.H. Wang, M.H. Wu, B.R. Bao et al., Study on hydrogen and CO produced by radiation degradation of *N*,*N*-dimethyl hydroxylamine. J. Radioanal. Nucl. Chem. **273**(2), 371–373 (2007). https://doi.org/10.1007/s10967-007-6842-7
30. H.L. Yale, The acetohydroxamic acid. Chem. Rev. **33**, 209–256 (1943)